Science Bulletin 64 (2019) 653–658

Contents lists available at ScienceDirect

Science Bulletin

journal homepage: www.elsevier.com/locate/scib

Article

Electric-field controlled superconductor-ferromagnetic insulator transition

Likuan Ma [a,1], Bin Lei [a,1], Naizhou Wang [a,1], Kaishuai Yang [b], Dayong Liu [b], Fanbao Meng [a], Chao Shang [a], Zeliang Sun [a], Jianhua Cui [a], Changsheng Zhu [a], Tao Wu [a,c,d], Zhe Sun [e,d], Liangjian Zou [b], Xianhui Chen [a,c,d,f,*]

[a] *Hefei National Laboratory for Physical Sciences at Microscale and Department of Physics, and CAS Key Laboratory of Strongly-coupled Quantum Matter Physics, University of Science and Technology of China, Hefei 230026, China*
[b] *Key Laboratory of Materials Physics, Institute of Solid State Physics, Chinese Academy of Sciences, Hefei 230031, China*
[c] *CAS Center for Excellence in Quantum Information and Quantum Physics, Hefei 230026, China*
[d] *Collaborative Innovation Center of Advanced Microstructures, Nanjing University, Nanjing 210093, China*
[e] *National Synchrotron Radiation Laboratory, University of Science and Technology of China, Hefei 230026, China*
[f] *CAS Center for Excellence in Superconducting Electronics (CENSE), Shanghai 200050, China*

ARTICLE INFO

Article history:
Received 20 March 2019
Received in revised form 12 April 2019
Accepted 12 April 2019
Available online 18 April 2019

Keywords:
FeSe-based superconductors
Ferromagnetic insulator
Phase transition
Solid ion conductor field-effect transistors (SIC-FET)

ABSTRACT

Superconductivity beyond electron-phonon mechanism is always twisted with magnetism. Based on a new field-effect transistor with solid ion conductor as the gate dielectric (SIC-FET), we successfully achieve an electric-field-controlled phase transition between superconductor and ferromagnetic insulator in (Li,Fe)OHFeSe. A dome-shaped superconducting phase with optimal T_c of 43 K is continuously tuned into a ferromagnetic insulating phase, which exhibits an electric-field-controlled quantum critical behavior. The origin of the ferromagnetism is ascribed to the order of the interstitial Fe ions expelled from the (Li,Fe)OH layers by gating-controlled Li injection. These surprising findings offer a unique platform to study the relationship between superconductivity and ferromagnetism in Fe-based superconductors. This work also demonstrates the superior performance of the SIC-FET in regulating physical properties of layered unconventional superconductors.

1. Introduction

The manipulation of collectively ordered electronic states is always the issue of long-standing focus in condensed matter physics. Many exotic electronic phases have been discovered with exertion of various methods including chemical doping and applying high pressure [1–4]. Chemical doping has triggered the finding of high-T_c superconductors by suppressing antiferromagnetism or spin density wave via introducing charge carriers in cuprates and iron-based superconductors, respectively [1–3]. In these systems, high-T_c superconductivity usually develops from antiferromagnetic insulators, and the high-T_c superconductivity and ferromagnetism are mutually exclusive [5,6]. The relationship of superconductivity and magnetism is a key for understanding of electron pairing mechanism beyond conventional electron-phonon superconductivity. Controlling magnetism at the vicinity of superconducting region could shed light on the investigation of the competing or intertwined electronic states in superconducting and magnetic phases.

Modulation of carrier density plays a critical role in the studies of superconductivity. In particular, this strategy can reveal the detailed evolution of various physical properties between superconductivity and magnetism in unconventional superconductors. An alternative approach to precisely control charge carrier concentration is the gating technique based on field-effect transistors (FETs) [7–9]. Through the electric-field-induced electrostatic doping with dielectric or electric-double-layer (EDL) surface gating via ionic liquid, electronic states of a two-dimensional system can be tuned continuously, and new electronic states could be realized beyond the limitation of conventional chemical doping [10–12]. However, these techniques could only tune the carrier density for thin flakes and the tuning depth is restricted to a few nanometers beneath the surface due to the Thomas-Fermi screening [13]. Recently, using solid ion conductor (SIC) as the gate dielectric, we have developed a type of FET device, namely SIC-FET [14–16]. Li ions can be driven into FeSe thin flakes with the SIC-FET, and

* Corresponding author.
E-mail address: chenxh@ustc.edu.cn (X. Chen).
[1] These authors contributed equally to this work.

https://doi.org/10.1016/j.scib.2019.04.022
2095-9273/

T_c = 8 K in pristine FeSe can be enhanced to 46 K. In addition, the $Li_xFe_2Se_2$ crystalline phase is stabilized by electric field and cannot be accessible by conventional methods [14].

In this paper, we successfully tune the electronic properties of (Li,Fe)OHFeSe thin flakes by electric field using the SIC-FET device. It is striking that a reversible transition from high-T_c superconductor to ferromagnetic insulator is realized by electric field. A dome-shaped superconducting phase diagram is mapped out, and T_c increases from 27 to 43 K at the optimal doping. In the phase diagram, there exists a quantum critical point, which separates high-T_c superconductor and ferromagnetic insulator. Such electric field control of magnetism is attracting the accumulative interest and could be potentially utilized for practical applications [17–22].

2. Experimental

High quality single crystals of pristine (Li,Fe)OHFeSe were grown by the hydrothermal reaction method. The (Li,Fe)OHFeSe thin flakes were mechanically exfoliated from pristine crystals and transferred onto the substrate surface of the solid ion conductor to fabricate SIC FET device. The thickness of the flakes was characterized by an atomic force microscopy (NX-10, Park system). Using the lithography and lift-off techniques, thin flakes (typically 120–200 nm thick) were patterned into a standard Hall bar configuration and coated with Cr/Au electrodes (5/150 nm) for transport measurements. The longitudinal resistance and *Hall* resistance were simultaneously measured in a six-probe *Hall* bar geometry using a commercial Quantum Design physical property measurement system (PPMS). The in-situ XRD data was collected by an X-ray diffractometer (SmartLab-9, Rikagu Corp.) with Cu K_α radiation. Detailed device fabrication and experimental measurements are described in the Supplementary materials (online).

3. Results and discussion

Fig. 1a is a schematic illustration of the SIC-FET device used in our studies. The exfoliated (Li,Fe)OHFeSe thin flakes with typical thickness of ~120 nm are used to fabricate the transport channel. The inset of Fig. 1b shows the optical image of a (Li,Fe)OHFeSe thin flake with a standard Hall bar configuration and with current and voltage terminals labeled. Li ions in the lithium ion conductor can be precisely controlled and driven into the thin flakes by electric field. Fig. 1b shows a typical *R*-V_g curve with a continuously sweeping rate of 1 mV s^{-1} at *T* = 260 K. The resistance of the sample remains almost unchanged with gating voltage for V_g > 4.25 V, and starts to drop evidently at V_g = 4.25 V, and reaches a minimum around V_g = 4.9 V, then increases drastically. When the gate voltage is swept back, the resistance continuously increases rapidly and then falls down. At V_g = −2 V, the resistance returns to a value close to the initial state. Such slight difference in resistance indicates that the Li injection-extraction cycle slightly changes microstructures, but the cycle controlled by electric field is highly repeatable.

Fig. 1c and d show the temperature dependent resistance of (Li,Fe)OHFeSe thin flake at various gate voltages. At V_g = 0 V, the (Li,Fe)

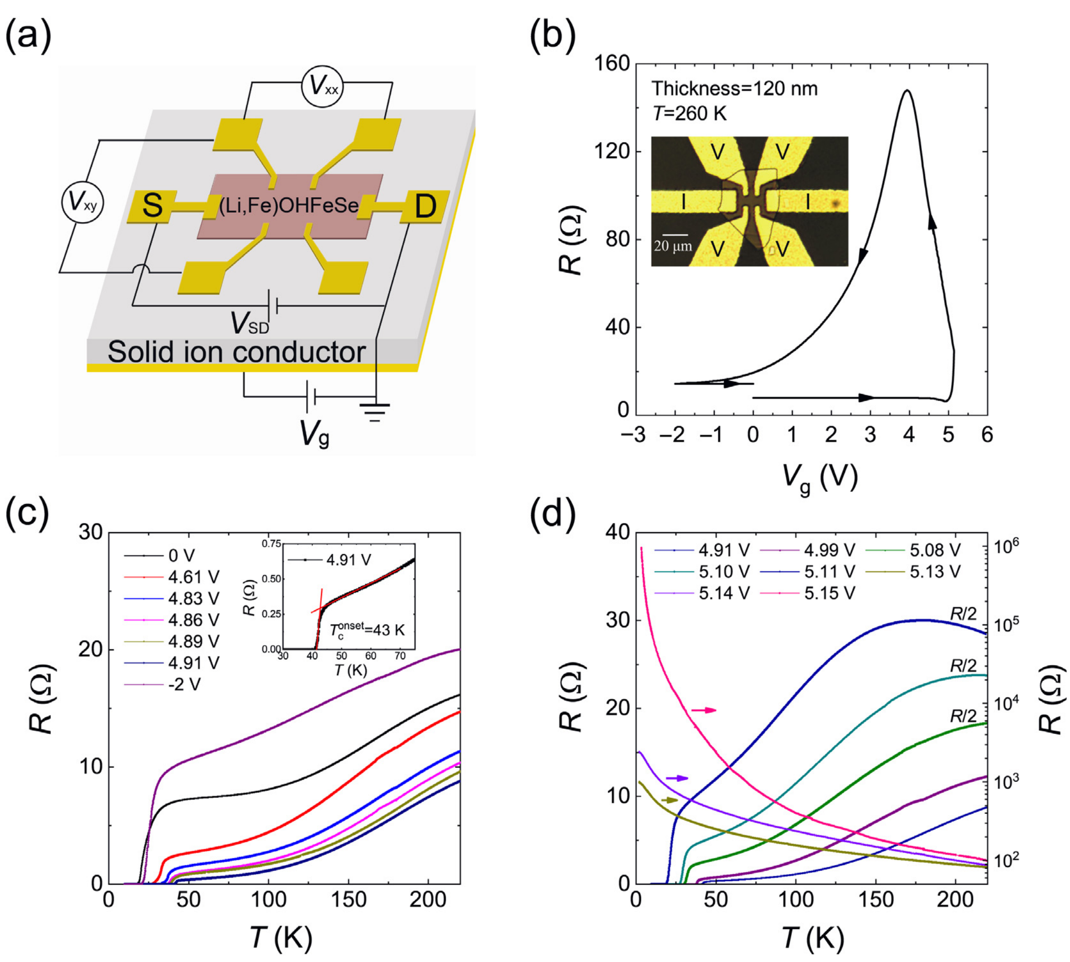

Fig. 1. Resistance of (Li,Fe)OHFeSe controlled by gate voltage with SIC-FET device. (a) A schematic view of the (Li,Fe)OHFeSe based SIC-FET device. From the bottom to the top: Cr/Au back gate layer, finely polished Li ion conductor substrate, (Li,Fe)OHFeSe thin flake and Cr/Au *Hall* bar electrodes. (b) Gate voltage dependent resistance of a (Li,Fe)OHFeSe thin flake with thickness of 120 nm in SIC-FET device. The inset shows the optical image of the device. (c) and (d) Temperature dependent resistance at different gating voltages.

OHFeSe thin flake shows superconductivity with an onset transition temperature T_c = 27 K. With increasing the gate voltage, Li ions are gradually driven into the sample, accompanied by an increase of T_c. When V_g = 4.91 V, the optimal superconductivity is achieved with T_c = 43 K, which is the same as the highest T_c in polycrystalline ($Li_{0.8}Fe_{0.2}$)OHFeSe [23]. With further increasing the Li content, T_c gradually decreases, and eventually the sample becomes an insulator. When the gate voltage is swept back to −2 V, superconductivity recovers and its T_c is close to the value before gating as shown in Fig. 1c. It further indicates that the gating process is reversible.

To further reveal the evolution of electronic properties in the gating process, the magnetic-field (H) dependent Hall resistance R_{xy} at T = 60 K is measured at different gating voltages. Fig. 2a and b show a linear magnetic-field dependence of Hall resistance in the superconducting regime. In contrast, it shows a superposition of a linear and a square-shaped hysteretic dependence in the insulating state as shown in Fig. 2c, indicating an anomalous Hall effect in the insulating state. Fig. 2d and e show H dependent Hall resistance and magnetoresistance at different temperatures. In Fig. 2d, the square-shaped hysteretic Hall resistance indicates that the sample is tuned to be a ferromagnetic insulator. In the ferromagnetic state, the total Hall resistance R_{xy} can be expressed as $R_{xy} = R_A M + R_H H$ [24,25], where R_A and R_H are the anomalous and ordinary *Hall* coefficients, respectively. M is the magnetization of the sample, and H is the external magnetic field. Fig. 2e illustrates H-dependent magnetoresistance (MR) measured at the corresponding temperatures, and a clear butterfly-shaped hysteresis arises, which is due to the spin-dependent scattering of carriers by local magnetic ordering. These results indicate the existence of a long-range ferromagnetic order in the insulating phase. The peak position in MR corresponds to the coercive field (H_c), and the reduced scattering of a specific spin orientation leads to negative MR on either side of H_c [25]. In both R_{xy}-H and MR curves, the smaller H_c at higher temperature suggests that the ferromagnetic order becomes much weaker with increasing temperature, which is a common characteristic in ferromagnetic materials [24]. It should be pointed out that these measurements are limited to the temperature below T = 175 K because the lithium ions could not be confined for T > 175 K. Moreover, our data suggest that the transition temperature of ferromagnetism (Curie temperature) should be much higher than 175 K, which cannot be determined in our measurements. In addition, the angular dependence of the MR is measured (Fig. S4 online). We find that the coercive field (H_c) increases with increasing the angle (θ) between the direction of the applied H and the c-axis of (Li,Fe)OHFeSe crystal. As shown in Fig. S4, H_c is proportional to $1/\cos\theta$. This behavior demonstrates that the easy axis of magnetization is along the c axis of (Li,Fe)OHFeSe with strong anisotropy. When the gate voltage is swept back to −2 V, H dependent Hall resistance recovers to a linear behavior,

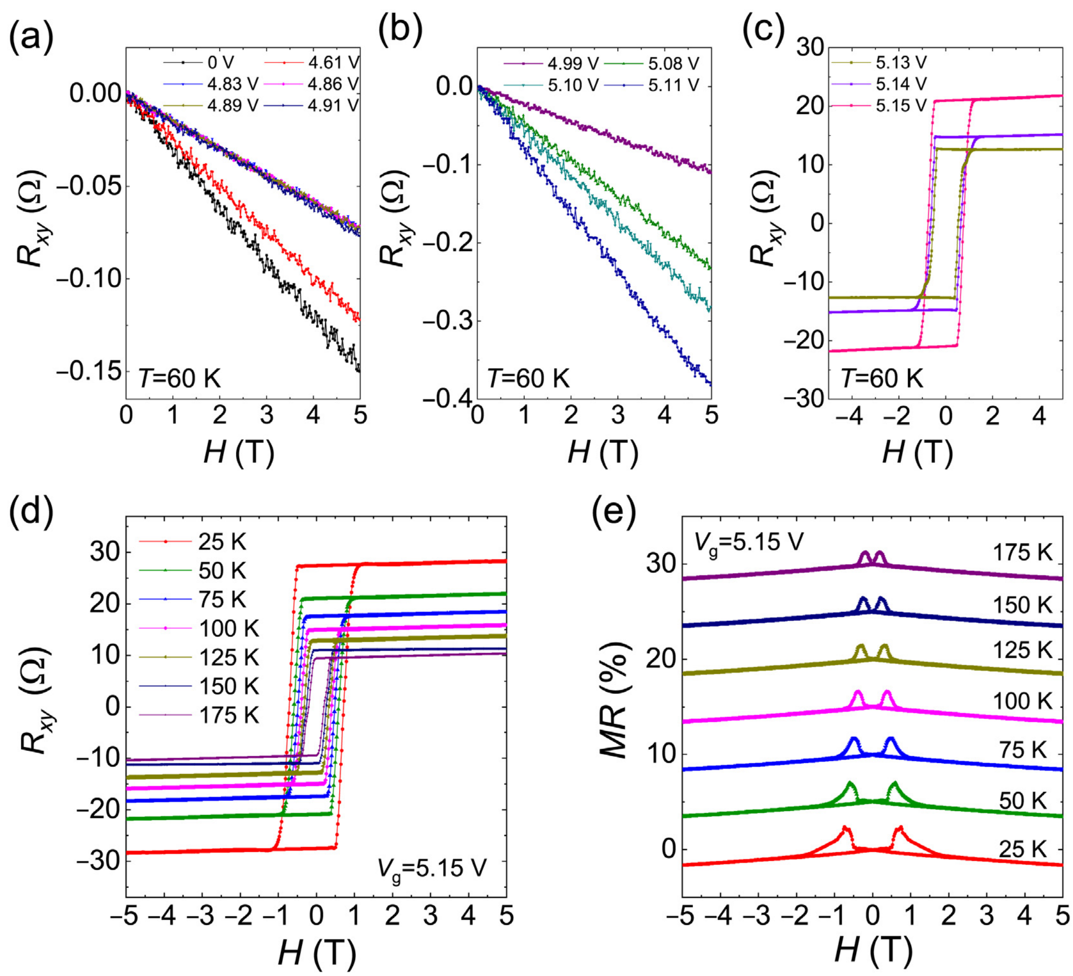

Fig. 2. The evolution of R_{xy}(H) with different gate voltage at T = 60 K, and R_{xy}(H) and MR(H) as a function of temperature at V_g = 5.15 V. (a) and (b) Magnetic field (H) dependent Hall resistance R_{xy} at 60 K with different gating voltages, $R_{xy}(H)$ shows linear behavior in the superconducting regime. (c) R_{xy} as a function of H at 60 K with different gating voltages, an obvious anomalous Hall effect is observed in the insulating regime. (d) and (e) Magnetic field dependent Hall resistance R_{xy} and magnetoresistance (MR) at different temperatures. The $MR(H)$ curves are shifted vertically with a step of 5% for clarity.

similar to the $R_{xy}(H)$ before gating without any anomaly (see Fig. S5b online). All these results indicate a superconducting-ferromagnetic insulating transition in (Li,Fe)OHFeSe with SIC-FET device, which can be reversibly controlled by electric field.

In-situ X-ray diffraction (XRD) is performed on the SIC-FET device at $T = 150$ K to study the structural evolution of (Li,Fe)OHFeSe thin flake, as shown in Fig. 3. We find that the injection of Li ions to the thin flake by electric field leads to structural modifications. The (0 0 1) diffraction peak of (Li,Fe)OHFeSe locates at $2\theta = 9.56°$ and 9.66° at $T = 300$ and 150 K before gating, respectively. With Li ions being driven into the thin flake by electric field, the (0 0 1) peak shows no noticeable variation in intensity and position until the gate voltage increases up to 4.91 V, at which the optimal T_c of 43 K is achieved. With further increasing the gate voltage, a new diffraction peak appears at lower angle of 8.44° (corresponding *d*-value of 10.48 Å), and it becomes stronger and shifts towards lower angle with increasing gate voltage. Concomitantly, the intensity of original (0 0 1) peak of (Li,Fe)OHFeSe gradually decreases. This result indicates a structural transformation from (Li,Fe)OHFeSe phase to a new structural phase induced by Li injection. When the gating voltage is increased to 5.24 V, the (Li,Fe)OHFeSe phase completely disappears, as shown in Fig. 3b. We note here that the coexistence of the (Li,Fe)OHFeSe phase and the new structural phase could be attributed to the inhomogeneity of the Li ions distribution. Such inhomogeneous distribution of Li ions in the sample is evidenced by the fact that the lattice parameter of *c*-axis for (Li,Fe)OHFeSe phase remains the same when the new structural phase shows up and grows as shown in Fig. 3. In addition, the inhomogeneous distribution of Li ions in the sample strongly depends on the thickness of the thin flake. It is possible that there is no coexistence of the two structural phases in a thinner flake. We have tried to perform XRD measurements on the device with the flake thickness less than 150 nm, but the sample is too thin (and too small) to yield decent diffraction signal.

We stress that there exist two kinds of evolution in XRD patterns during gating as the gate voltage is sweeping backwards to −2 V as shown in Figs. 3 and S2 (online), respectively. The former occurs in an irreversible gating process, while the latter takes place in a reversible process. In Fig. 3, the (0 0 1) diffraction peak of the new structural phase shifts from 8.02° to 8.92° (corresponding *d*-value from 11.02 to 9.91 Å) when the gate voltage varies from 5.29 to −2 V. The *d*-value of 9.91 Å is much larger than that (9.21 Å) of the original (Li,Fe)OHFeSe phase. It suggests that the gating process is irreversible. Such an irreversibility is also confirmed in electric transport. When V_g varies from 5.29 to −2

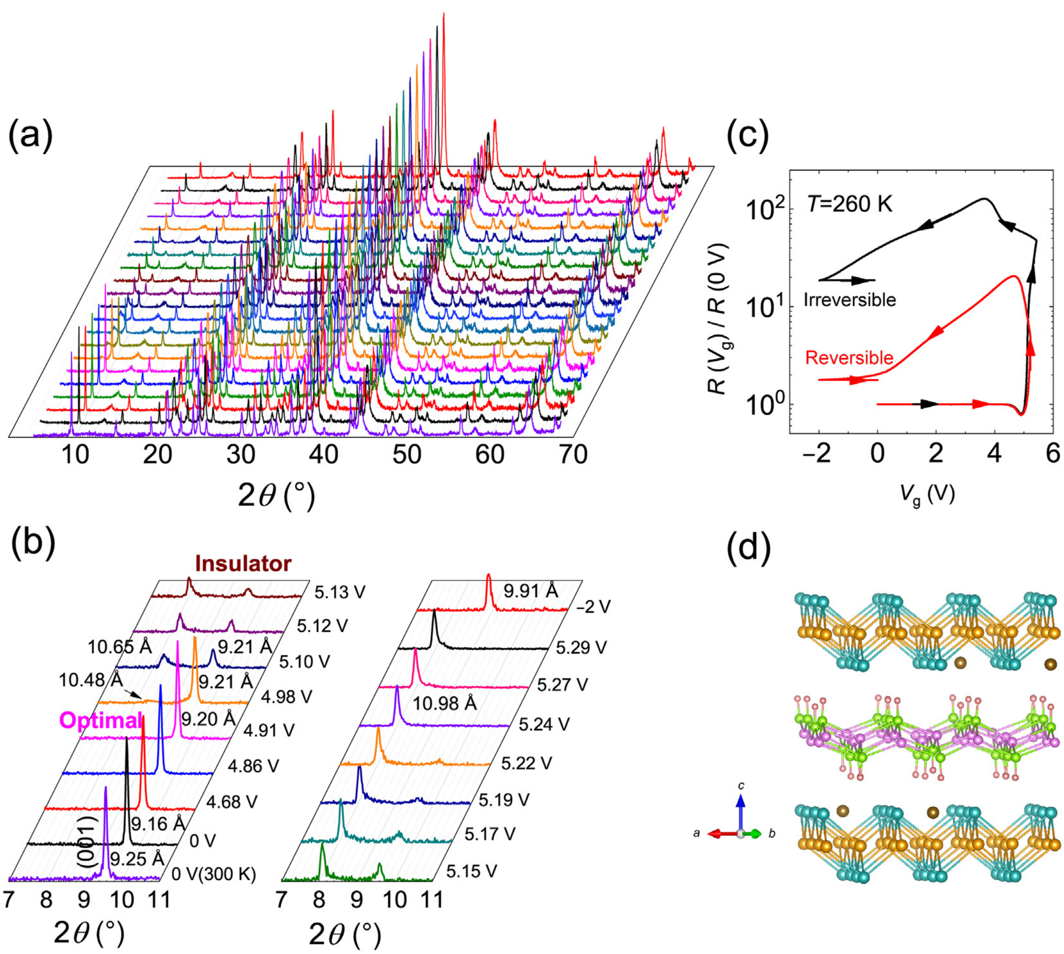

Fig. 3. In-situ X-ray diffraction patterns of (Li,Fe)OHFeSe thin flake at various gate voltages in the SIC-FET device. (a) In-situ XRD patterns of (Li,Fe)OHFeSe thin flake with thickness of 175 nm under different V_g at $T = 150$ K. The XRD pattern taken at 300 K before gating is also plotted. Since the sample is thin flake of single crystal with (0 0 *l*) orientation, only (0 0 1) and (0 0 2) diffraction peaks for original structure and (0 0 1) diffraction peak for the new structure can be observed. All other diffraction peaks are from the solid lithium ion conductor substrate, Au electrode and vacuum chamber, and are marked by different symbols in the Fig. S8 (online). (b) The magnified view of the angle range from 7° to 11°. The corresponding *c*-axis lattice parameters at some gate voltages are labeled beside the diffraction peak. (c) The gate voltage dependent $R(V_g)/R$ (0 V) of (Li,Fe)OHFeSe thin flake for reversible (red) and irreversible (black) process in the SIC-FET device at $T = 260$ K. (d) Calculated crystalline lattice configurations with $a = b = 8.1854$ Å, $c = 10.1792$ Å (space group: *P4/n*) for the $Fe_{0.2}LiOHFeSe$ phase.

V, the resistance is one order magnitude larger than that before gating as shown in Fig. 3c; in addition, the thin flake shows insulating behavior, in contrast to superconducting behavior before gating as shown in Fig. S5c (online). However, in the reversible gating process, the diffraction peak of the new structural phase shifts from 8.21° to 9.35° (corresponding *d*-value from 10.77 to 9.46 Å) when the gate voltage is swept from 5.14 to −2 V as shown in Fig. S2 (online), and the *d*-value of 9.46 Å is close to that (9.21 Å) of the original (0 0 1) diffraction peak of (Li,Fe)OHFeSe phase. This behavior indicates that the gating process is nearly reversible, which is evidenced both by the gating curve in Fig. 3c and by the recovery of superconductivity with nearly the same T_c from a ferromagnetic insulating state in Fig. S5a (online). These results indicate that the newly formed structural phase is stabilized only by electric field and that whether the gating process controlled by electric field is reversible or not strongly depends on the maximal voltage applied in the gating process.

Based on the transport and in-situ XRD measurements, the phase diagram for the gate-voltage tuned (Li,Fe)OHFeSe thin flake is plotted in Fig. 4. At $V_g = 0$ V, the (Li,Fe)OHFeSe thin flake shows superconductivity with $T_c = 27$ K. As listed in Table S1 (online), the composition of the thin flake obtained by structural refinement is $(Li_{0.81}Fe_{0.19})OHFe_{0.97}Se$. The existence of Fe vacancies in the selenide layers is responsible for the low-T_c of 27 K [26,27]. Li ions are gradually driven into the thin flake by electric field, and T_c shows a dome-like behavior. The optimal superconductivity with $T_c = 43$ K is achieved when the gate voltage is increased to 4.91 V, which is the same as that of $(Li_{0.8}Fe_{0.2})OHFeSe$ [23]. With further increasing the gate voltage, T_c gradually decreases, and then the superconductivity is completely suppressed, and eventually the system goes into a ferromagnetic insulator. It is striking that there exists a quantum critical point at the gating voltage of 5.13 V, which separates superconducting and ferromagnetic insulating state. As shown in Fig. 4, the lattice parameter of *c*-axis for (Li,Fe)OHFeSe phase monotonically increases with increasing the gate voltage up to 4.91 V, then saturates with further increasing the gate voltage, accompanied by the appearance of a novel structural phase with (0 0 1) diffraction peak at $2\theta = 8.44°$. The *c*-axis lattice parameter of the novel structural phase monotonously increases with increasing the gate voltage. There exists a boundary between reversibility and irreversibility for the gating process around $V_g = 5.18$ V, and the gating process is irreversible for $V_g > 5.18$ V. It should be addressed that coexistence of high-T_c superconductivity and ferromagnetic state in the same phase diagram is observed for the first time.

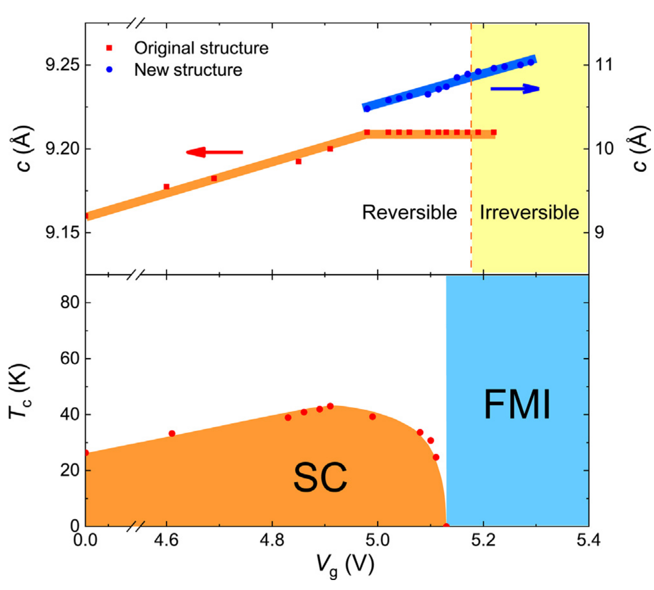

Fig. 4. The phase diagram of the gate-tuned (Li,Fe)OHFeSe thin flake. The T_c at different gate voltages is determined by the onset critical temperature T_c^{onset} from the resistance measurements. The *c*-axis lattice parameter is determined by the position of (0 0 l) peaks from the in-situ XRD patterns. The dashed line at $V_g = 5.18$ V indicates the boundary between the reversible and irreversible gating regimes.

We propose a scenario of the lithiation process controlled by electric field to explain these findings in (Li,Fe)OHFeSe thin flake, which is also supported by first-principles calculations as will be shown later. Fe in the (Li,Fe)OHFeSe phase has two different crystallographic positions, Fe1 is in the selenide layers and Fe2 is in (Li,Fe)OH layers. Li ions driven into (Li,Fe)OHFeSe thin flake prefer to enter into the (Li,Fe)OH layer and replace the Fe2. As listed in Table S1 (online), the starting material is $(Li_{0.81}Fe_{0.19})OHFe_{0.97}Se$ with $T_c = 27$ K. When the Li ions are initially driven into the thin flake, Li ions replace the Fe in the hydroxide layers and the Fe ions expelled by Li can migrate away from the hydroxide layers to fill the vacancies in the selenide layers. Once the vacancies are filled, the thin flake achieves the optimal $T_c \sim 43$ K. Similar lithiation process has been observed in hydrothermally synthesized $(Li_{1-x}Fe_x)OHFe_{1-y}Se$ polycrystalline powder lithiated with *n*-BuLi lithiating reagent [27]. The Fe ions further extruded from the hydroxide layers migrate to the interstitial sites, which is evidenced by the appearance of new structure reflections just after the optimal doping achieved, as shown in Fig. 3. When the amount of the aggregated Fe reaches a certain value, the interstitial Fe ions become ordered and eventually lead to a long-range ferromagnetic order. As soon as the Fe in the hydroxide layer is completely replaced by Li, the thin flake is a ferromagnetic insulator with composition of $Fe_{0.16}LiOHFeSe$. When V_g is swept back to −2 V, Fe ions at the interstitial sites can re-occupy the original positions in (Li,Fe)OH layer, leading to the disappearance of ferromagnetic state and the recovery of superconductivity (see Fig. S5a and S5b online). With further driving Li ions into the thin flake, there exist two possible cases. One is that Li may expel the Fe from the selenide layer as pointed out by Woodruff et al. [27]. Another is that the extra Li ions distribute in the interstitial sites. In either way, the gating process is irreversible when the V_g is swept backwards from 5.29 to −2 V, so that the new structure cannot transform back to the (Li,Fe)OHFeSe phase. This is the reason why the device shows an insulating behavior without ferromagnetism (see Fig. S5c and S5d online).

In order to understand the new crystal structure and reversibility during the Li gating process, first-principle calculations is performed to search for the most stable atomic configurations and crystalline structures. We find that Li ions driven into thin flake by electric field prefer to replace Fe in (Li,Fe)OH layer and expel Fe out of the (Li,Fe)OH layer to the interstitial sites. The Fe ions expelled from the hydroxide layers migrate to the center of the Se square of FeSe layer, and optimized stable structure with $c = 10.18$ Å is obtained for the new structural phase with $Fe_{0.2}LiOHFeSe$ as shown in Fig. 3d. A similar location of excess Fe has been observed in $Fe_{1+x}(Te,Se)$ by STM [28]. The potential barrier for the Fe ions expelled by Li ions from the hydroxide layer to the interstitial site of FeSe layer is about 0.16 eV, and it is about 0.45 eV for the reversal process (see Fig. S7 online). The process with such a low potential barrier is easily reversible. On the other hand, we also explore the possibility of Li substitution for the Fe in the selenide layer after Fe ions in (Li,Fe)OH layer are completely replaced. We consider two situations: Li occupation in interstitial site or Li substitution for Fe in the FeSe layers. We find that the total energy of the latter is about 2.3 eV higher than the former, ruling out the possibility of Li substitution for Fe in the FeSe layers. In one word, the theoretical calculations not only qualitatively explain the experimental observations, but also predict the structure of the novel metastable crystalline phase.

4. Summary

In summary, we can control the crystal structural transformation with electric field through SIC-FET, and the corresponding electronic and magnetic states are regulated simultaneously. High-T_c superconductivity and ferromagnetism rarely exist simultaneously in the same phase diagram, and it is thus striking to realize the control of phase transition by electric field from high-T_c superconducting state to ferromagnetic insulating state. Our study demonstrates the potential applications of the SIC-FET for multifunctional devices and its superior tunability for an electronic system that transcends the ability of carrier doping. These findings open a new way for the control of magnetic and electronic states, and pave a way to access the metastable phases and to find the unexpected physical properties.

Conflict of interest

The authors declare that they have no conflict of interest.

Acknowledgments

This work was supported by the National Key R&D Program of China (2017YFA0303001 and 2016YFA0300201), the Strategic Priority Research Program (B) of the Chinese Academy of Sciences (XDB25010100), the National Natural Science Foundation of China (11888101 and 11534010), Science Challenge Project (TZ2016004) and Hefei Science Center CAS (2016HSC-IU001).

Author contributions

X.H.C. conceived and coordinated the project, and is responsible for the infrastructure and project direction. L.K.M., B.L., N.Z.W. contributed equally to this work. L.K.M., L.B. and N.Z.W. performed device fabrication and measurements with assistance from C.S., F. B.M., Z.L.S., J.H.C., C.S.Z., Z.S., K.S.Y., D.Y.L. and L.J.Z. performed theoretical analysis and calculations. L.K.M., B.L., N.Z.W., T.W. and X.H. C. analyzed the data. X.H.C., L.K.M., B.L., N.Z.W. and Z.S. wrote the paper. All authors discussed the results and commented on the manuscript.

Appendix A. Supplementary data

Supplementary data to this article can be found online at https://doi.org/10.1016/j.scib.2019.04.022.

References

[1] Bednorz JG, Müller KA. Possible high T_c superconductivity in the Ba–La–Cu–O system. Z Phys B 1986;64:189–93.
[2] Kamihara Y, Watanabe T, Hirano M, et al. Iron-based layered superconductor $LaO_{1-x}F_xFeAs$ (x = 0.05–0.12) with T_c = 26 K. J Am Chem Soc 2008;130:3296–7.
[3] Chen XH, Wu T, Wu G, et al. Superconductivity at 43 K in $SmFeAsO_{1-x}F_x$. Nature 2008;453:761.
[4] Gor'kov LP, Kresin VZ. Colloquium: high pressure and road to room temperature superconductivity. Rev Mod Phys 2018;90:011001.
[5] Lee PA, Nagaosa N, Wen XG. Doping a Mott insulator: physics of high-temperature superconductivity. Rev Mod Phys 2006;78:17.
[6] Dai PC. Antiferromagnetic order and spin dynamics in iron-based superconductors. Rev Mod Phys 2015;87:855.
[7] Ahn CH, Bhattacharya A, Ventra MD, et al. Electrostatic modification of novel materials. Rev Mod Phys 2006;78:1185.
[8] Bisri SZ, Shimizu S, Nakano M, et al. Endeavor of iontronics: from fundamentals to applications of ion-controlled electronics. Adv Mater 2017;29:1607054.
[9] Saito Y, Kasahara Y, Ye JT, et al. Metallic ground state in an ion-gated two-dimensional superconductor. Science 2015;350:409.
[10] Caviglia AD, Gariglio S, Reyren N, et al. Electric field control of the $LaAlO_3$/$SrTiO_3$ interface ground state. Nature 2008;456:624.
[11] Ueno K, Nakamura S, Shimotani H, et al. Discovery of superconductivity in $KTaO_3$ by electrostatic carrier doping. Nat Nanotech 2011;6:408.
[12] Ye JT, Zhang YJ, Akashi R, et al. Superconducting dome in a gate-tuned band insulator. Science 2012;338:1193.
[13] Ueno K, Shimotani H, Yuan HT, et al. Field-induced superconductivity in electric double layer transistors. J Phys Soc Jpn 2014;83:032001.
[14] Lei B, Wang NZ, Shang C, et al. Tuning phase transitions in FeSe thin flakes by field-effect transistor with solid ion conductor as the gate dielectric. Phys Rev B 2017;95:020503(R).
[15] Zhu CS, Cui JH, Lei B, et al. Tuning electronic properties of $FeSe_{0.5}Te_{0.5}$ thin flakes using a solid ion conductor field-effect transistor. Phys Rev B 2017;95:174513.
[16] Ying TP, Wang MX, Zhao ZY, et al. Discrete superconducting phases in FeSe-derived superconductors. Phys Rev Lett 2018;121:207003.
[17] Ohno H, Chiba D, Matsukura F, et al. Electric-field control of ferromagnetism. Nature 2008;408:944.
[18] Shiota Y, Nozaki T, Bonell F, et al. Induction of coherent magnetization switching in a few atomic layers of FeCo using voltage pulses. Nat Mater 2012;11:39.
[19] Matsukura F, Tokura Y, Ohno H. Control of magnetism by electric fields. Nat Nanotech 2015;10:209.
[20] Huang B, Clark G, Klein DR, et al. Electrical control of 2D magnetism in bilayer CrI_3. Nat Nanotech 2018;13:544.
[21] Wang Z, Zhang TY, Ding M, et al. Electric-field control of magnetism in a few-layer van der Waals ferromagnetic semiconductor. Nat Nanotech 2018;13:554.
[22] Deng YJ, Yu YJ, Song YC, et al. Gate-tunable room-temperature ferromagnetism in two-dimensional Fe_3GeTe_2. Nature 2018;563:94.
[23] Lu XF, Wang NZ, Wu H, et al. Coexistence of superconductivity and antiferromagnetism in $(Li_{0.8}Fe_{0.2})OHFeSe$. Nat Mater 2015;14:325.
[24] Zhang ZC, Feng X, Guo MH, et al. Electrically tuned magnetic order and magnetoresistance in a topological insulator. Nat Commun 2014;5:4915.
[25] Checkelsky JG, Lee MH, Morosan E, et al. Anomalous Hall effect and magnetoresistance in the layered ferromagnet $Fe_{0.25}TaS_2$: the inelastic regime. Phys Rev B 2008;77:014433.
[26] Sun HL, Woodruff DN, Cassidy SJ, et al. Soft chemical control of superconductivity in lithium iron selenide hydroxides $Li_{1-x}Fe_x(OH)Fe_{1-y}Se$. Inorg Chem 2015;54:1958.
[27] Woodruff DN, Schild F, Topping CV, et al. The parent Li(OH)FeSe phase of lithium iron hydroxide selenide superconductors. Inorg Chem 2016;55:9886.
[28] Yin JX, Wu Z, Wang JH, et al. Observation of a robust zero-energy bound state in iron-based superconductor Fe(Te, Se). Nat Phys 2015;11:543.

Likuan Ma obtained his B.S. degree from Northeast Normal University (NENU) in 2014, and then became a graduate student in the University of Science and Technology of China under the supervision of Prof. Xianhui Chen. His current research interest focuses on tuning novel physical properties and phase transitions between different quantum states using field-effect.

Xianhui Chen obtained his Ph.D. degree in physics from the University of Science and Technology of China (USTC) in 1992. In the same year, he began his research career in USTC and now holds the position of Professor in Physics. His research is focused on the exploration and study of the physics of novel functional materials exhibiting superconductivity, novel magnetism, novel quantum properties, thermoelectricity, etc.